Thermal stabilization of the Large Millimeter Telescope

F. Peter Schloerb[a], Kamal Souccar[a], David M. Gale[b], Xia Huang[a], Andrea León Huerta[b], David H. Hughes[b], José Luis Hernández Rebollar[b], and Grant W. Wilson[a]

[a]Department of Astronomy, University of Massachusetts, Amherst Massachusetts, USA
[b]Instituo Nacional de Astrofísica, Óptica, y Electrónica, Tonantzintla, Puebla, Mexico

ABSTRACT

External environmental conditions lead to thermal deformations of the primary reflector of the 50-m diameter Large Millimeter Telescope Alfonso Serrano (LMT). This paper describes efforts to improve the night-time performance of the telescope at millimeter-wavelengths and allow extension of scientific observations into daylight hours, using the LMT's active surface to counteract the effects of thermal gradients within the antenna structure. Several approaches to stabilizing the LMT's thermal behavior will be described, including operation of a ventilation system in the antenna backup structure and a real-time metrology system to measure and correct large-scale, thermally induced, surface deformations.

Keywords: Radio Telescopes, Thermal Behavior of Radio Telescopes, Millimeter-wave Telescopes, Antenna Surface Deformation, Telescope Alignment, Telescope Design

1. INTRODUCTION

The Large Millimeter Telescope Alfonso Serrano (LMT) is a 50m-diameter radio telescope for millimeter-wave astronomy (Figure 1). Large telescopes like the LMT are usually limited in their ultimate performance by transient, thermally induced, deformations, and because of this, the LMT is only rarely operated outside of nighttime hours. This paper describes our efforts to reduce the impact of thermal gradients and eventually permit routine observations during daytime hours, when differential solar heating of the structure leads to significant deformations. The thermal stabilization program is also expected to lead to improvements during nighttime hours, when cooling of the structure creates temperature gradients and causes the surface to deform during the night. The LMT is equipped with an active primary surface which may be adjusted to remove any deformations that may arise. Thus, a primary goal of the program is estimation of the shape of the surface in real time so that corrections can be made.

Figure 1. Views of the Large Millimeter Telescope at its site atop Sierra Negra in the state of Puebla, Mexico. The location of the telescope is shown in the right-hand panel.

The program described here is the continuation of a long term effort at the LMT to improve its overall performance.[1–3] In this paper, we will summarize several initiatives underway at LMT to upgrade the antenna

Further author information: (Send correspondence to F.P.S)
F.P.S: E-mail: schloerb@umass.edu

Ground-based and Airborne Telescopes X, edited by Heather K. Marshall, Jason Spyromilio, Tomonori Usuda, Proc. of SPIE Vol. 13094, 130940P
 · 0277-786X · doi: 10.1117/12.3018497

systems and permit scientific observations under all thermal conditions. These include: (1) design and installation of a ventilation system for the antenna backup structure to minimize thermal gradients; (2) improved temperature sensing and finite element modeling of the structure; (3) calibration of the finite element models with photogrammetric measurements; (4) use of astronomical observations to measure surface shape in real time; and (5) development of *LASERS* — a high precision laser ranging system to measure secondary position and surface shape in real time.

2. LMT DESIGN

2.1 LMT Structure

The main structural components of the LMT are identifed in Figure 2. The antenna is a wheel-on-track mount with an alidade which rotates about the vertical axis. The Azimuth Rotating Structure (ARS) is identifed in the figure and consists of the Alidade Base (AB) and upper part of the alidade (UA). The AB and UA are large box beam structures fabricated with thick (35 mm) steel plate. The exterior of the alidade structure is covered with insulating cladding.

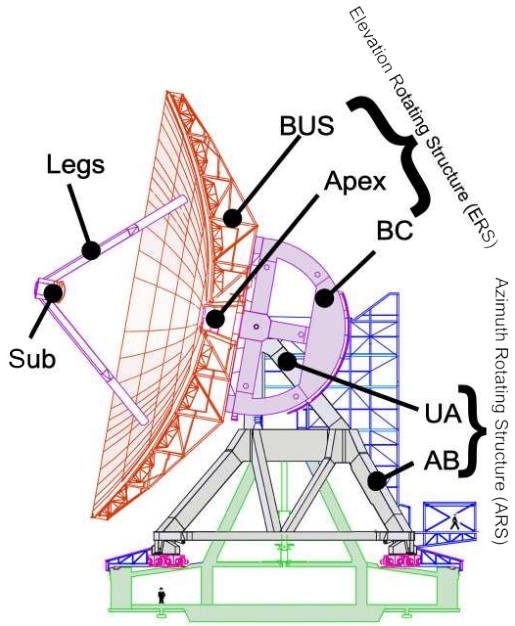

Figure 2. Identifcation of structural components of the Large Millimeter Telescope.

The Elevation Rotating Structure (ERS) is comprised of all parts of the antenna that are rotated in elevation about a horizontal axis to allow the antenna to point at any location on the sky. This consists of a steel spaceframe backup structure (BUS) to which the antenna's reflector segments are attached. The BUS consists of cylindrical beams of varying thickness from 20mm for the largest beams in the inner part of the BUS to about 5mm for thinner beams in the outer part. The BUS is enclosed by insulating cladding. The BUS is built around a fabricated steel cone, known as the Apex Cabin (Apex). The cone is a substantial structure with 22mm thick steel plate. The BUS is attached to a pair of counter weights, known as the "Ballast Cantilevers" in the LMT nomenclature (BC). These are also fairly massive structures fabricated with, typically, 17mm thick plate. The BC's are filled with concrete to provide the counterweight to the main reflector.

The reflector surface itself consists of 180 trapezoidal surface segments. Each segment has 8 precision surface panels which are aligned on the segment's structure in the laboratory and then installed with the segment on the antenna. Segments are placed in five concentric rings with Ring 1 as the innermost ring and Ring 5 as the outermost. Each segment has four actuators, one at each corner of the segment, to allow the antenna surface

to be adjusted for shape changes due to gravitational and thermal loads. Finally, the secondary mirror of the antenna's optical system (subreflector) is located near the focus of the main parabola. It is held in position by four support legs (the tetrapod) attached to the BUS in the middle of the fourth ring of segments.

The LMT was designed with an active primary surface. This feature allows the antenna to adjust its surface to respond to changes in shape that may arise due to gravitational and/or thermal loading. Gravitational loading is a function of elevation only and does not change for other reasons. Accordingly, it is straightforward, in principle anyway, to measure the shape of the surface at different elevation angles and program actuator motions to compensate for this deformation. On the other hand, deformations arising from thermal gradients within the structure are transient in nature and require development of other approaches to enable real time correction with the active surface.

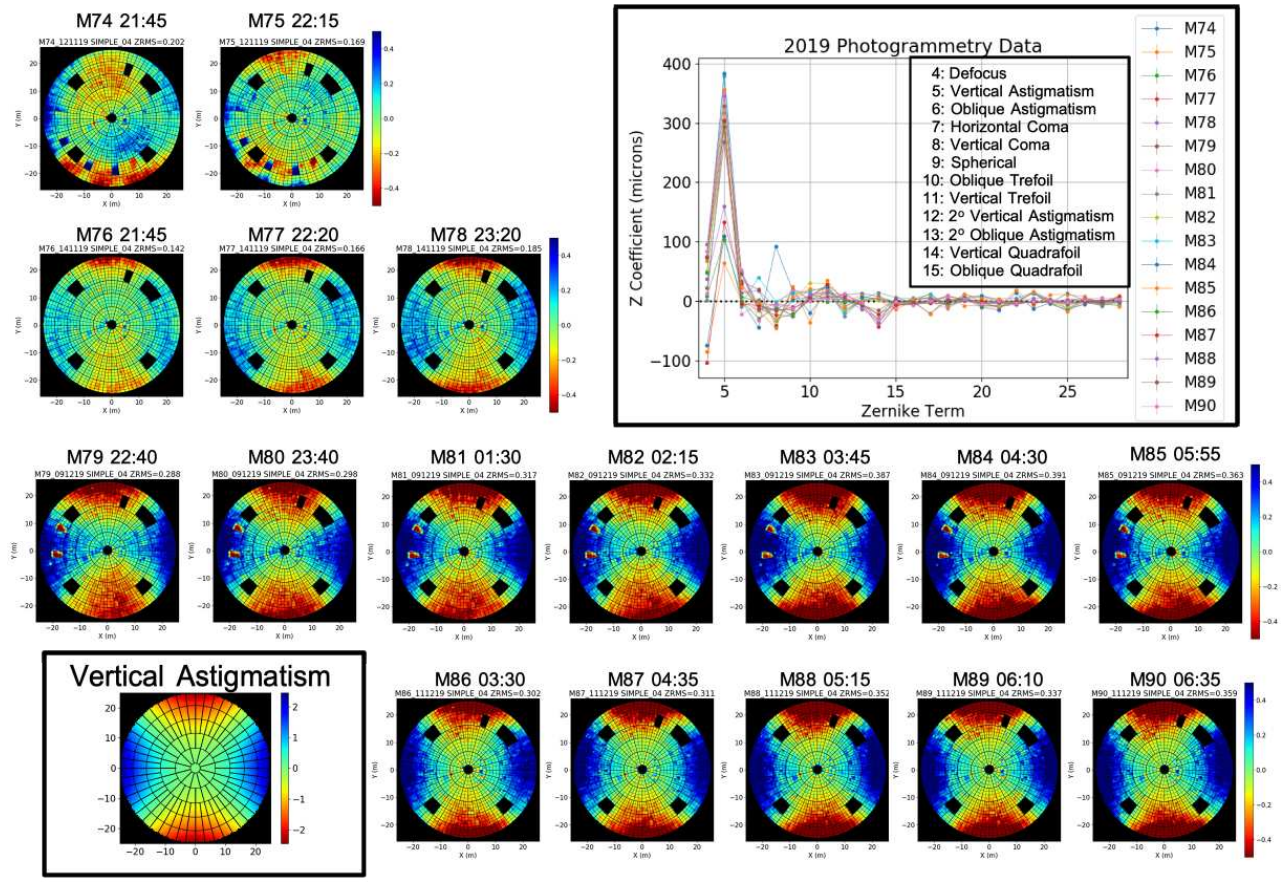

Figure 3. LMT photogrammetry maps obtained during the fall of 2019. The maps were obtained by positioning the antenna at a fixed elevation and simply repeating the mapping procedure through the night. Each row in the figure presents observations on a different night. The inset figure plots the coefficients of Zernike polynomials required to fit all maps. The largest terms, as may be evident from inspection of the maps, are the defocus and vertical astigmatism polynomials. In general, the surface is well characterized by low order deformations.

2.2 Thermal Deformations of the LMT Structure

Thermal deformations of the LMT surface may be directly measured using photogrammetry, as described in Gale et al[4] and Schloerb et al.[3] Figure 3 ilustrates a previous result of this work where the antenna was measured repeatedly during the night while fixed in position. Each row in the figure represents a different night of measurements, and we note that there are changes in the surface shape from night to night as well as within individual nights of measurements. The surface shape for all maps has been characterized using Zernike

polynomials, and the results of these fits are shown in the inset figure. A basic conclusion about the structure is that the largest deformations of the surface occur in the defocus and vertical astigmatism polynomials. It is also important to emphasize that the complete surface can be well characterized by the first 14 Zernike terms, so that corrections with the active surface do not need to consider terms of higher order.

Finite element models of the LMT structure provide basic information on the nature of deformations that arise from thermal gradients within the structure. Figure 4 illustrates the results for several cases of structural temperature gradients. Inspection of the patterns indicates that the patterns observed by photogrammetry can be explained by simple temperature differences between stuctural elements of the LMT.

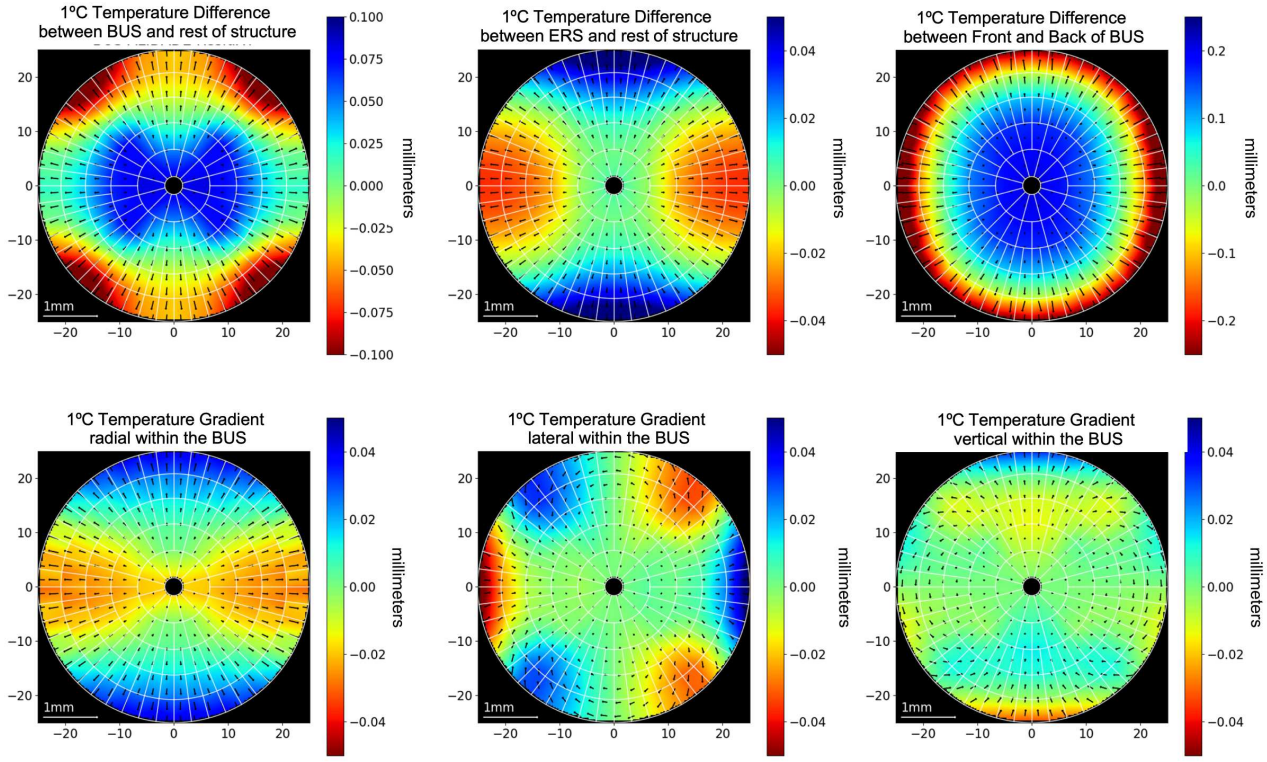

Figure 4. FEM results of thermal cases for the LMT Structure. The figures portray deformations along the optical axis of the parabola in color, using the color scale bars shown. Vectors on the surface show the direction and magnitude of predicted motions perpendicular to the optical axis and are scaled according to the one-millimeter scale bar on the image. Thermal cases are (clockwise from top left): (1) 1°C temperature difference between BUS and the rest of the structure; (2) 1°C temperature difference between elevation rotating structure (see Figure 2) and the rest of the structure; (3) 1°C difference between top chord and bottom chord of BUS; (4) 1°C vertical gradient within the BUS; (5) 1°C linear lateral gradient within the BUS; (6) 1°C linear radial temperature gradient within the BUS.

2.3 LMT Active Surface

The 50m-diameter aperture of the LMT is comprised of 180 trapezoidal surface segments. The segments are designed to be independently adjusted using actuators positioned at the four corners. The active surface is a key part of the LMT design for two reasons. First, as noted above, it is possible to correct for gravitational deformations of the structure through use of a look-up table. The second use of the active surface is to respond to transient errors in its shape due to thermal deformations. However, to make use of this capability, we require a way to measure the shape of the surface in real time so that the corrections can be made. We will describe

various ways that are being developed for this purpose in the next section of the paper (*Mitigation of Thermal Deformations*).

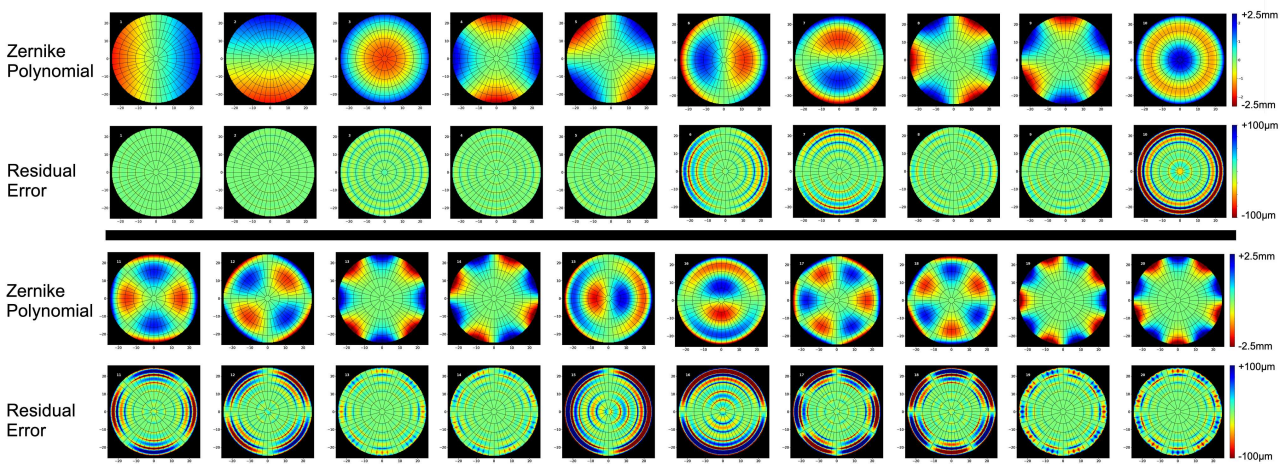

Figure 5. LMT Active Surface ability to produce Zernike Polynomial patterns.

A feature of the active surface is that there are limits on its ability to replicate deformations of the antenna at all scales. To illustrate this, we show, in Figure 5, the ability of the surface to replicate deformations according to patterns that follow Zernike Polynomials. The panels in the figure show the deformation along with the residuals to a fit of the active surface to the Zernike polynomial. The residual errors are small for the lowest order Zernike terms (vertical tilt, horizontal tilt, defocus, vertical astigmatism, and oblique astigmatism). However, for slightly higher order terms illustrated in the figure (horizontal coma, vertical coma, and spherical aberration), there are errors at the level of a few percent of the original deformation at some places on the surface. Even higher order Zernike deformations, through secondary spherical aberration, lead to larger errors at the level of 10% of the original deformation. The largest errors are located primarily in the outer rings of segments on the surface since the higher order Zernike polynomials vary rapidly near the edge of the aperture.

3. MITIGATION OF THERMAL DEFORMATIONS

3.1 BUS Ventilation System

The LMT's backup structure (BUS) is enclosed in cladding to block direct sunlight from the structure and provide insulation to moderate environmental temperature changes. The original design of the LMT called for installation of a ventilation system in the BUS to reduce thermal gradients caused by uneven heating or ponding of warm air trapped within the enclosed BUS at the top of the structure. However, this system was not installed at the time of the completion of telescope construction. During the past year, the project has moved ahead toward accomplishing this goal.

A detailed design of the BUS ventilation system has been completed by B2Q Associates (Andover Massachusetts USA). The design is based on a similar system which has been in use on the IRAM 30m telescope for many years[5] The system designed for LMT is comprised of 10 radial ducts. Each duct has a fan located near the center of the BUS to force air radially outward. The air is forced out of the lefthand side of the radial ducts in order to promote a counterclockwise airflow of about 4 m/s in the BUS. The rate of airflow through the system is 180,000 cubic meters per hour. The LMT's ducts will be fabric ducts to lower the overall system weight. At this time, the LMT is planning for the acquisition and installation of the necessary components of the B2Q design.

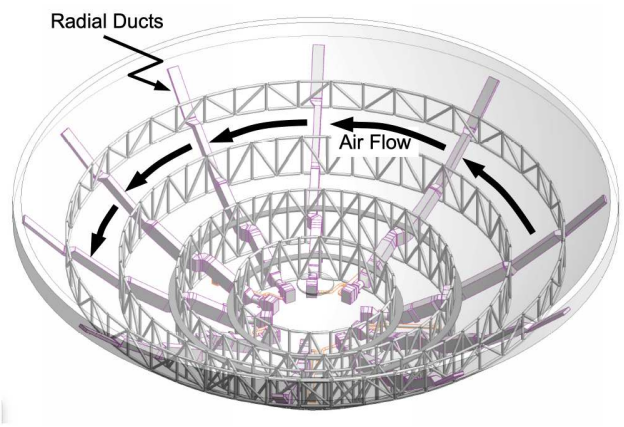

Figure 6. The LMT BUS Ventilation System. The system is comprised of 10 radial ducts which promote airflow in a counterclockwise direction aroung the LMT BUS..

3.2 Thermal Sensing System

The original temperature sensing system on the LMT had a total of about 60 sensors within the BUS and on the rest of the structure. Measurements with these sensors, over many years, permitted the characterization of the antenna's response to solar heating and temperature changes in the environment.[2] Nevertheless, accurate finite element modeling of the structural response to thermal gradients requires more complete sampling of the structural members than was possible with this small number of sensors. Therefore, a new set of temperature sensors have been procured and tested in our laboratory in preparation for installation on the telescope.

A total of 269 4-wire RTD temperature sensors and their associated readout hardware has been acquired and tested in the labs at UMass. The sensors will have an absolute accuracy of about 0.2°C. The error is almost entirely a systematic offset of the readout from individual sensors. The offset is due to: (1) variations in sensor manufactured resistance within the variation specification (about 0.1°C); and (2) meter errors in the readout system (also about 0.1°C). Despite a significant attempt to remove these effects using calibrated resistors, we have found that there are apparently too many variables at work to achieve a simple calibration. Thus, in the actual system, there will be small sensor to sensor offsets. We have found, in evaluation of our current system, that there are times at the telescope when the structure becomes nearly isothermal, which might allow the offsets to be estimated. We have also found that the important thing for tracking thermal effects is measurement of *changes* in the difference in temperature between structural elements, which is not affected by individual sensor offsets.

3.3 Calibration of Finite Element Models with Photogrammetry Measurements

With improved temperature sensing of the structure and the ability to make accurate measurements of the antenna surface with photogrammetry,[4] the INAOE metrology group is able to make detailed comparisons of changes in the shape of the surface in response to temperature changes within the structure. Our ability to carry out this work was illustrated in Figure 3, which shows results derived from of photogrammetry maps of the surface made during a night when the antenna surface was measured repeatedly for several hours. Recently, we have made use of data like this to compare observed changes to predictions of the FE model.

Figure 7 shows an example of such a comparison. A map of changes in the surface shape, measured by the difference between the first and last maps made during a night, was fit to the FE model to derive temperature differences within the structure. The effects considered included differences between major structural elements and low order gradients within the BUS, similar to those illustrated in Figure 4. The model provides a good fit to the change in shape that is observed, with the main temperature changes found by the model corresponding generally to observed cooling of the BUS and the Ballast Cantilevers during the night. However, the magnitude of the changes required by the thermal model is a few times larger than the observed temperature changes. We

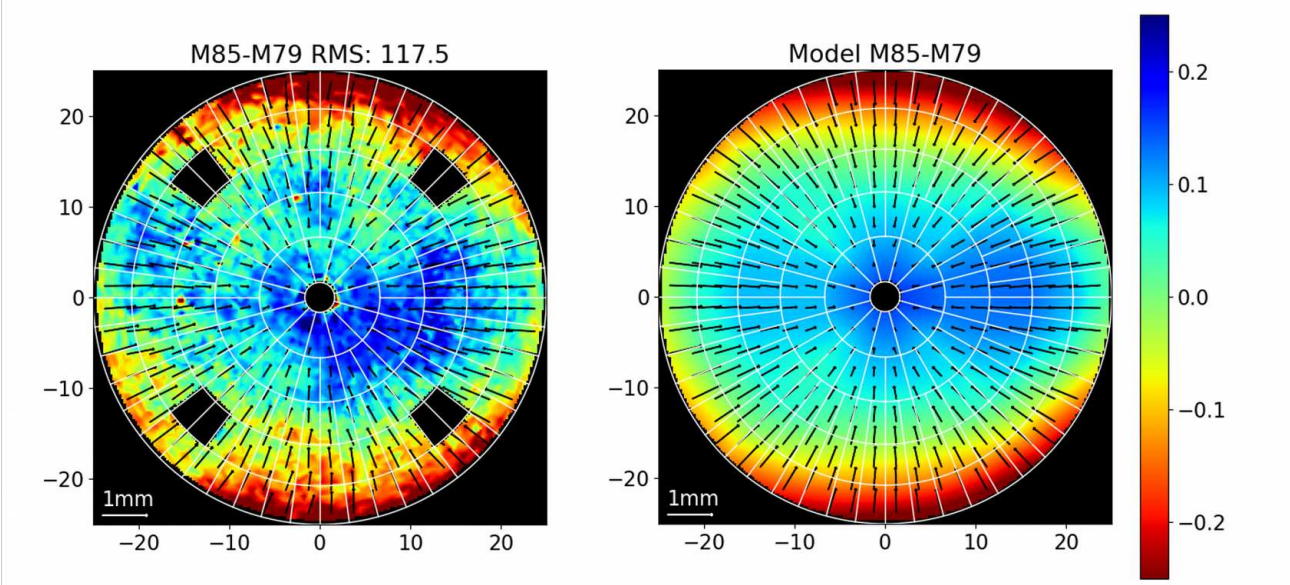

Figure 7. Left: Measurement of the difference between a photogrammetry map made at the end of a night of measurements and the first photogrammetry map made that night. (See third row of Figure 3.) The difference map renders changes along the optical axis on a color scale. Changes in the surface perpendicular to the optical axis are shown as vectors, scaled according to the scale bar in the figure. Right: Results of a model fit to the difference map at left. The model accounts for temperature differences between major structural elements and low order gradients within the BUS.

believe that this quantitative discrepancy may be due to the limited temperature sensor coverage of the structure by our old system, and we look forward to repeating experiments like this once the new sensor system is installed. Our long term goal for this work is to calibrate the FEM with actual surface measurements in order to enable prediction of the surface shape from structural temperature measurements.

3.4 Surface Measurement through Astronomical Observations

Observations of the antenna surface with photogrammetry[2,4] have revealed that a major transient feature, shaped like the Zernike polynomial for vertical astigmatism, changes from night to night and within individual nights at the telescope. Based on the thermal cases shown in Figure 4, it is clear that the structure deforms to this shape under a variety of thermal stresses, owing to the nature of the bearings on the two ballast cantilevers that provide the attachment points between the antenna BUS and the alidade.

Understanding that the major transient changes to the shape of the antenna are in the focal length and the vertical astigmatism shape, it is useful to find ways to estimate the magnitude of these effects during the course of normal observations. Optimization of the antenna focus using the secondary mirror is, of course, a standard part of observing. The active surface of the LMT allows a simple assessment of other changes in the optical system, as described by Schloerb et al.[1]

At LMT, our operational routine includes a procedure to optimize the value of the coefficient of the Zernike vertical astigmatism polynomial. This is done by making a sequence of measurements of the antenna gain after programming the astigmatism polynomial shape into the surface with different values of the coefficient. Figure 8 shows a typical run made at 3.5mm wavelength. This simple measurement technique allows one of the major shape deformations to be measured in real time during observations.

In addition to the straightforward procedure outline above, it is also possible to solve for focus and vertical astigmatism shape as well as higher order Zernike polynomials using the out-of-focus (OOF) holography technique.[6,7] In this technique, beam patterns are measured with the secondary mirror at different positions along the optical axis. The beam patterns may then be fit to a set of functions describing the phase variations along the antenna surface. Usually, the Zernike polynomials are used to represent the phase variations, although in

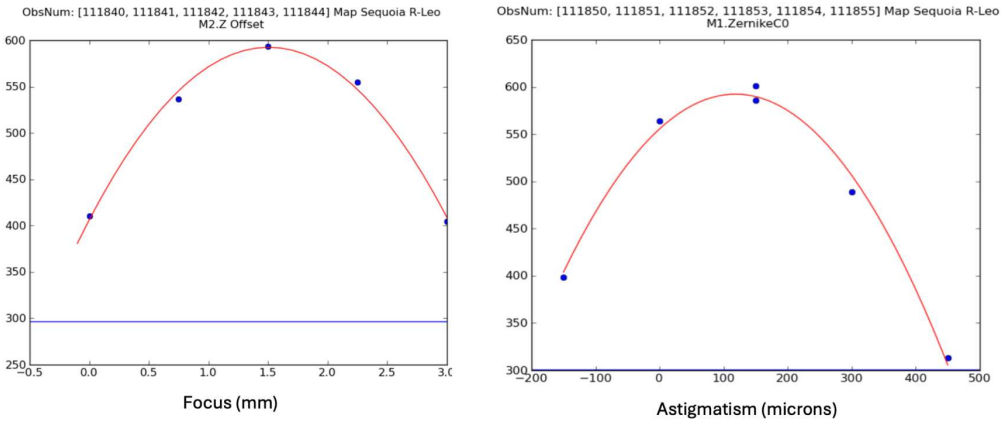

Figure 8. Left: A focus curve measured at 3.5mm at the LMT. Right: A curve showing the change of antenna gain as different values for the vertical astigmatism coefficient are programmed into the active surface. The measurements are an easy way to optimize the two major shape changes that occur at LMT due to thermal gradients within the structure.

our model, we also solve for the best secondary position (in place of the Zernike defocus polynomial). As noted previously, photogrammetry measurements at LMT during night time conditions show that the major transient deformations can be represented by low order Zernike polynomials, which makes the OOF technique a potentially powerful one.

To prepare for an operational role for the OOF procedure at LMT, we have analyzed a number of routine focus measurements made at the telescope with our OOF program. A typical focus measurement uses a set of beam patterns to determine the peak flux at different secondary focus positions. The maps are usually limited to an area just outside of the main beam and are therefore not well suited for determination of high order deformations of the surface by the OOF technique. However, they contain excellent information about the lower orders and are especially sensitive to the astigmatism term.

To illustrate the progress with the OOF procedure, we present data obtained using the J=2-1 v=1 SiO Maser in the star R Leo. This bright source provides a signal-to-noise ratio in excess of 1000 for the map, and allows good OOF results to be obtained. Figure 9 shows a set of measured beam patterns at different focus positions across the top row. Model beam patterns, corresponding to simple OOF model fits, are shown in the two lower rows. The middle row presents a model which includes only one Zernike polynomial (vertical astigmatism) in addition to secondary position and pointing error terms. The bottom row includes additional Zernike polynomials beyond vertical astigmatism including: oblique astigmatism, vertical and horizonal coma, vertical and oblique trefoil, and spherical aberration. Inclusion of the additional terms improves the model fit significantly, but the beam pattern measurements do not extend far enough from the main lobe of the pattern to allow fully reliable determination of the higher order Zernike terms from this data.

Figure 10 illustrates a comparison of the focus and astigmatism results measured on March 6, 2024 UT at LMT using our normal operational method, illustrated in Figure 8, and the OOF analysis of the maps obtained for the focus measurement. The OOF model (labeled "5p" in the figure) is the simplest one, which makes a solution for pointing, secondary position, and vertical astigmatism. Results of the two methods agree well and justify the use of the OOF method during future operations.

3.5 Real Time Measurement of the Surface with *LASERS*

A final approach to dealing with transient deformations of the antenna is to measure the LMT surface and secondary position in real time, so that corrections can be made using the active surface or the secondary mirror positioning system. Schloerb at al[3] described the LMT's approach to making measurements of the telescope using a commercial laser ranging system from Hexagon DEU01 GmbH. This work was inspired by pioneering work carried out by Rakich and collaborators at the Large Binocular Telescope[8] using the same laser ranging instrument to provide a "laser metrology truss" for active optics systems on the LBT.

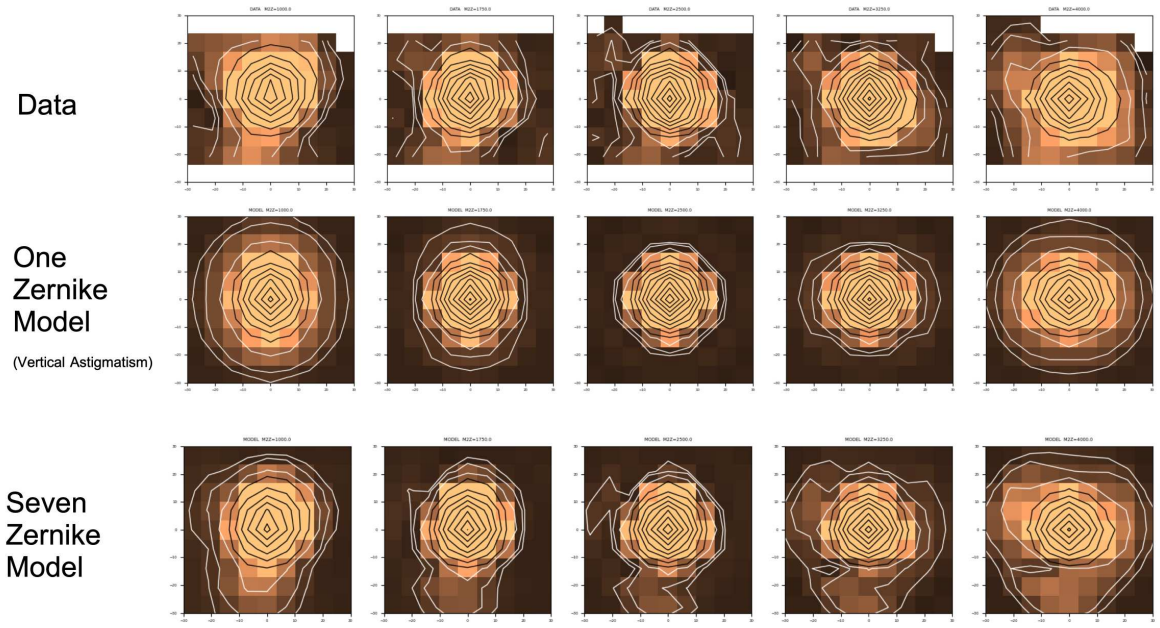

Figure 9. Small beam pattern maps taken during a routine focus observation at LMT. The top set of maps show the actual data. OOF model fits which include the Zernike vertical astigmatism term and not other, higher order Zernike terms are shown in the middle row. The bottom row illustrates a fit using Zernike polynomials with higher order up the the spherical aberration term.

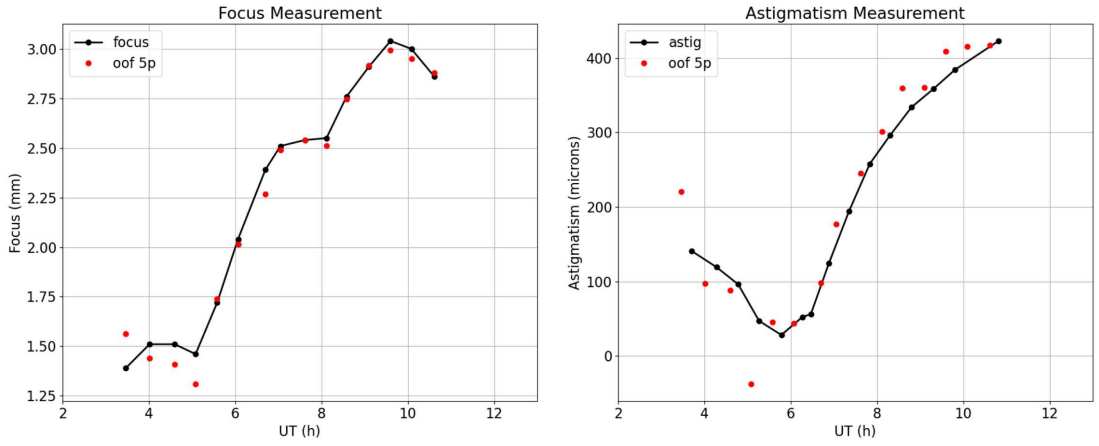

Figure 10. Left: Results of OOF analysis for best secondary position compared to result of a focus determination made in the traditional manner. Right: OOF results for the vertical astigmatism parameter compared to measurements of vertical astigmatism made using the technique illustrated in Figure 8. OOF results in both cases are derived from a fit of beam patterns made at different secondary positions along the optical axis and solve for secondary position, vertical astigmatism and possible pointing offsets.

The LMT's metrology system project — the Large Aperture Surface Error Recovery System (*LASERS*) — is underway with the acquisition of the laser ranging instrument under funding from the US National Science Foundation Major Research Instrumentation Program. Tests of the device in the laboratory, reported on by Schloerb et al,[3] show that the instrument met its basic specification of a relative distance measurement error of 5×10^{-7} under lab conditions over the ∼20m ranges needed at the LMT. Subsequent work has demonstrated successful measurements under turbulent conditions outside the laboratory, which is a positive result for our exposed telescope in sunlight conditions. Unfortunately, progress towards installation has been slowed by technical problems with the instrument which required its return to Hexagon in Germany for resolution. We believe that we are on track for return of the instrument in 2024 so that installation, testing, and commissioning can begin.

ACKNOWLEDGMENTS

We acknowledge the effort of the LMT metrology team at INAOE for their work on antenna photogrammetry and system testing of the Hexagon AMT device: Maribel Lucero Álvarez, Esteban Tecuapetla Sosa, David Castro Santos, Carlos Tzile Torres, and Emilio Hernández Rios.

This work would not have been possible without the long-term financial support from the Mexican Humanities, Science and Technology Funding Agency, CONAHCYT (Consejo Nacional de Humanidades, Ciencias y Tecnologías), and the US National Science Foundation (NSF), as well as the Instituto Nacional de Astrofísica, Óptica y Electrónica (INAOE) and the University of Massachusetts, Amherst (UMass). The operation of the LMT is currently funded by CONAHCYT grant #297324 and NSF grant #2034318.

FPS also acknowledges: (1) the Next Generation Event Horizon Telescope Design Project (NSF AST-1935980) for support of his efforts devoted to LMT thermal characterization, thermal modeling, and the development of real-time measurement concepts; and (2) support from the NSF Major Research Instrumentation Program (NSF AST-2117422) for the acquisition of the Hexagon AMT instrument and support of the installation and commissioning of the system.

REFERENCES

[1] Schloerb, F., Sanchez, D., Narayanan, G., Erickson, N., Souccar, K., Wilson, G., Gale, D., Hughes, D., and Smith, D., "Calibration and operation of the active surface of the large millimeter telescope," in [*Ground-based and Airborne Telescopes VI*], H. J. Hall, R. G. and Marshall, H. K., eds., *Proc. SPIE* **9906**, 99066C (2016).

[2] Schloerb, F., Souccar, K., Dagostino, M. C., Rodriguez, D., Gale, D., Gomez-Ruiz, A., Huerta, A. L., Hughes, D., Sanchez-Arguelles, D., and Wilson, G., "Moving towards daytime observing at the large millimeter telescope," in [*Ground-based and Airborne Telescopes VIII*], H.K. Marshall, J. S. and Usuda, T., eds., *Proc. SPIE* **11445**, 1031–1046 (2020).

[3] Schloerb, F., Souccar, K., Gale, D., Huerta, A. L., Hughes, D., and Wilson, G., "Lasers: a real time antenna metrology system for the large millimeter telescope," in [*Advances in Optical and Mechanical Technologies for Telescopes and Instrumentation V*], Ramón Navarro, R. G., ed., *Proc. SPIE* **12188**, 1218819 (2022).

[4] Gale, . D., Schloerb, F., Huerta, A. L., Álvarez, M. L., Cuevas, L. C., Sosa, E. T., Santos, D. C., Torres, C. T., and Rios, E. H., "Photogrammetry mapping and alignment of the lmt 50-meter primary reflector," in [*Advances in Optical and Mechanical Technologies for Telescopes and Instrumentation III*], Ramón Navarro, R. G., ed., *Proc. SPIE* **10706**, 1070646 (2018).

[5] Baars, J., Greve, A., Hooghoudt, B., and Penalver, J., "Thermal control of the iram 30m millimeter radio telescope," *Astron. Astrophys.* **195**, 364–371 (1987).

[6] Nikolic, B., Hills, R., and Richer, J., "Measurement of antenna surfaces from in- and out-of-focus beam maps using astronomical sources," *Astron. Astrophys.* **465**, 679–683 (2007).

[7] Nikolic, B., Prestage, R., Balser, D. S., Chandler, C. J., and Hills, R. E., "Out-of-focus holography at the green bank telescope," *Astron. Astrophys.* **465**, 685–693 (2007).

[8] Rakich, A., Choi, H., Veillet, C., Hill, J., Kuhn, O., Bec, M., Zhang, Y., Brendelb, T., Sitarski, B., and Schoenell, W., "Commissioning a laser metrology truss for active optics on the large binocular telescope," in [*Ground-based and Airborne Telescopes IX*], H.K. Marshall, J. Spyromillio, T. U., ed., *Proc. SPIE* **12182**, 121820D (2022).